Journal of Alloys and Compounds 509 (2011) 1054–1059

Contents lists available at ScienceDirect

Journal of Alloys and Compounds

journal homepage: www.elsevier.com/locate/jallcom

Effects of heat treatment scheme on the photocatalytic activity of TiO_2 nanotube powders derived by a facile electrochemical process

Yulong Liao, Wenxiu Que*, Zhenhua Tang, Wenjuan Wang, Wenhan Zhao

Electronic Materials Research Laboratory, School of Electronic and Information Engineering, Xi'an Jiaotong University, Xi'an 710049, Shaanxi, PR China

ARTICLE INFO

Article history:
Received 24 August 2010
Received in revised form
23 September 2010
Accepted 26 September 2010
Available online 23 October 2010

Keywords:
TiO_2 nanotube
Heat treatment
Phase structure
Photocatalytic activity

ABSTRACT

TiO_2 nanotubes (NTs) in powder form were synthesized by a facile electrochemical process in a perchlorate-containing electrolyte. Transmission electron microscopy results indicate that the TiO_2 NT-powder is in an amorphous structure and has outer diameter of 20 nm and tube-wall thickness of 5 nm. X-ray diffraction analysis reveals that phase composition of the annealed TiO_2 NT-powders is related to the heat treatment scheme. Methyl orange was employed as a representative dye pollutant to evaluate the ultraviolet photocatalytic activity of the TiO_2 NT-powders. It was found that different post heat treatment schemes affect greatly the photocatalytic activities of the TiO_2 NT-powders, which should be ascribed to the changes in phase structural and morphological properties of the TiO_2 NT-powders. These results indicate that there should be a balance between crystal phase and nanotubular configuration for achieving the best photocatalytic activity of the TiO_2 nanotube powders.

© 2010 Elsevier B.V. All rights reserved.

1. Introduction

Titanium dioxide (TiO_2) is one of metal oxide semiconductors, which owns outstanding chemical stability, high refraction index, great ultraviolet absorptivity, and photochemical activity [1–3]. It has been widely utilized in many scientific and technological areas including biomedical science, photocatalysis, photovoltaic solar cells, fuel cells, gas sensors, photonic crystals, ceramics, ultraviolet blockers, smart coating, and inorganic membrane [4–10]. Recently, one dimensional (1-D) TiO_2 nanostructures, such as nanotubes, nanobelts, and nanowires, have attracted much attention [11,12], because of the new physical and chemical properties when the size of the material reaches to nanometer scale.

As has been reported that nanotubular TiO_2 owns a better photochemical reactivity than bulk TiO_2 particles, due to not only the large specific surface area but also the nanotubular architecture providing channels for enhanced electron transfer [13,14]. TiO_2 nanotubes (NTs) can be synthesized by different methods, including anodization, template-assisted growth, hydrothermal, self-assembly, and sol–gel methods [15–20]. Particularly, the anodic oxidation process has shown to be a facile method to synthesize TiO_2 NTs. In our previous work, TiO_2 NTs were synthesized by the anodization of titanium foil into powder form in a perchlorate containing aqueous electrolytes [21]. The as-synthesized TiO_2 NT-powder is only amorphous and has about 20 nm in outer diameter and 5 nm in tube-wall thickness. Thus, the amorphous TiO_2 NT-powder needs to be crystallized so that they can be used in photocatalysis. TiO_2 owns three crystal structures, namely anatase, rutile and brookite. Among them, rutile phase has the highest refractive index and ultraviolet absorptivity, thus it has wide applications in pigments, paints, ultraviolet absorbents [22]. On the other hand, anatase phase is not only chemically but also optically active, which is suitable for catalysts and supports [23]. Usually, these two crystal phases have their own stabilization temperature ranges and can be affected by heat treatment schemes [24].

In this work, two different heat treatment schemes were adopted to the post annealing of the TiO_2 NT-powders. One heat treatment scheme was carried out at a relatively slow heating and cooling rate, while another scheme was designed at a sudden heating and cooling strategies. The aim of this work is to examine the effects of the heat treatment schemes on the crystal phase and the photocatalytic activity of the TiO_2 NT-powder derived from rapid anodization, which is expected to provide a further understanding for the physical and chemical properties of the TiO_2 NT-powders.

2. Experimental

2.1. Preparation of TiO_2 NT-powders

Raw titanium (Ti) sheet was anodized into the form of TiO_2 NT-powder by a two-electrode electrochemical process as we reported earlier [21]. Briefly, a piece of Ti foil (4 cm × 4 cm, 99.5% purity, 0.2 mm in thick) was anodized into powder form in 0.15 M $HClO_4$ aqueous solution at 25 °C, here, a platinum (Pt) foil was used as the counter electrode. The anodization voltage was kept at 20 V across the electrodes (2.5 cm between two electrodes) with the help of a DC power supply (Model GPS-

* Corresponding author. Tel.: +86 29 82668679; fax: +86 29 82668794.
E-mail address: wxque@mail.xjtu.edu.cn (W. Que).

0925-8388/$ – see front matter © 2010 Elsevier B.V. All rights reserved.
doi:10.1016/j.jallcom.2010.09.175

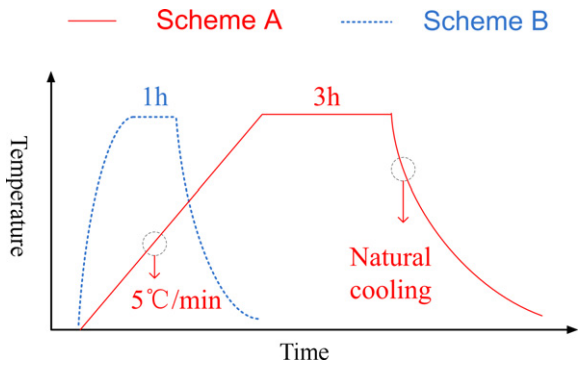

Fig. 1. Schematic diagrams of two different heat treatment schemes.

3303c, GW Instrument Co., Ltd, Taiwan). After a series of subsequent processing, the white TiO_2 NT-powders were obtained.

In order to achieve well-defined crystalline structures, followed the as-prepared TiO_2 NT-powders were annealed in muffle furnace under two different heat treatment schemes, denoted as Scheme A and Scheme B. Fig. 1 shows the schematic diagram of the two different heat treatment schemes. For Scheme A, the samples were heated to the target temperature (300, 450, and 550 °C) at a relatively slow heating-rate (5 °C/min) at first, and then kept the temperature at the target values for 3 h, finally the samples were naturally cooled to room temperature. For Scheme B, the samples were directly put into the muffle furnace which had been heated to the target temperatures (300, 450, 500 and 550 °C), after 1 h later, the samples were directly taken out of the furnace and finally cooled to room temperature in air.

2.2. Characterization

Transmission electron microscopy (TEM, JEM2100, JEOL Inc., Japan) was used to characterize the structural and morphological properties of the TiO_2 NT-powders. The X-ray diffraction (XRD) patterns of the TiO_2 NT-powders were obtained by a D/max-2400 X-ray diffraction spectrometer (Rigaku) with Cu Kα radiation, which operated at 40 kV and 100 mA from 20° to 70° with the scanning speed of 15°/min and step of 0.02°. The concentration of the methyl orange (MO) aqueous solution was measured by the UV–Vis absorption spectrum from JASCO V-570 UV/VIS/NIR spectrometer at a wavelength of 465 nm.

2.3. Photocatalytic activity measurement

To evaluate the photocatalytic activity, a degradation process of the methyl orange (MO, $C_{14}H_{14}N_3NaO_3S$) aqueous solution was investigated using a high-pressure mercury lamp (300 W) as light source. 20 mg/L MO aqueous solution was selected as the photocatalytic probe. The annealed TiO_2 NT-powders of 300 mg/L were suspended into the MO aqueous solution by ultrasonic dispersion at first, and then the mixture of the suspension (100 mL, PH: about 7.0) was put in dark with a stirring to ensure adsorption–desorption equilibrium prior to ultraviolet irradiation. Subsequently, the photocatalytic degradation was carried out by stirring the reaction mixture under ultraviolet irradiation. Certain volume of the suspension solution was withdrawn at a sequence of time intervals. After centrifugation, the residual MO aqueous solution was measured by the UV–Vis spectrophotometer at 463 nm based on the Beer–Lambert Law [25]:

$$\mathrm{Abs} = \varepsilon bc \quad (1)$$

where Abs is the measured absorbance, ε is the wavelength-dependent molar absorptivity coefficient, b is the path length, and c is the analyte concentration, thus $c/c_0 = A/A_0$ can be easily obtained, where c_0 is the initial concentration of the MO aqueous solution, A_0 is the initial absorbance value of the MO aqueous solution. Another set of testing, in which no any photocatalyst was added, was carried out as the blank test.

3. Results and discussion

3.1. TEM characterization

Fig. 2 shows the TEM image of the TiO_2 NT-powders, which were synthesized in the 0.15 M $HClO_4$ aqueous electrolyte at 25 °C. It can be observed that the obtained TiO_2 NTs are about several micrometers in length and consist of many highly ordered individual TiO_2 nanotubes. Upper inset of Fig. 2 shows the TEM image of the TiO_2 NT-powder with a higher magnification, and it can be found that the outer diameter and the tube wall thickness of the NTs are about 20 nm and 5 nm, respectively. Moreover, it can be also clearly observed that the as-synthesized TiO_2 NTs show a hollow structure and have a smooth outer and inner surface. Downside inset of Fig. 2 shows the selected area electron diffraction (SAED) pattern of the TiO_2 NTs, which indicates that the as-synthesized TiO_2 NT-powders have no crystallization and show an amorphous structure. These results are good in line with what we reported previously.

3.2. Crystalline and photocatalytic properties of the TiO_2 NT-powders annealed by Scheme A

Fig. 3 shows the XRD patterns of the TiO_2 NT-powders annealed by Scheme A at 300, 450, and 550 °C, respectively. It can be seen that all the studied samples are well crystallized after a heat treatment. For the TiO_2 NT-powders annealed at 300 °C, only some characteristic peaks that match with the reflection planes of the anatase

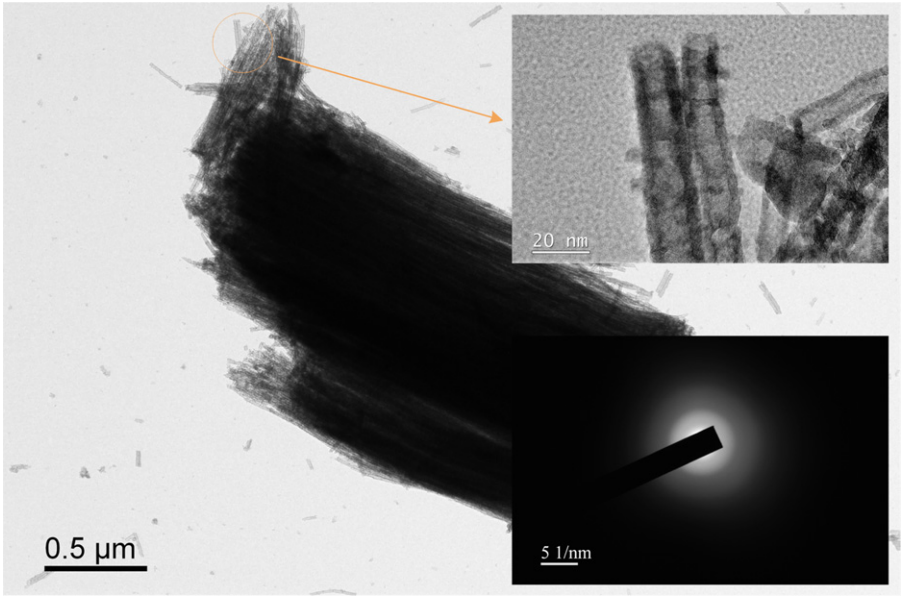

Fig. 2. TEM image of the as-synthesized TiO_2 NT-powders.

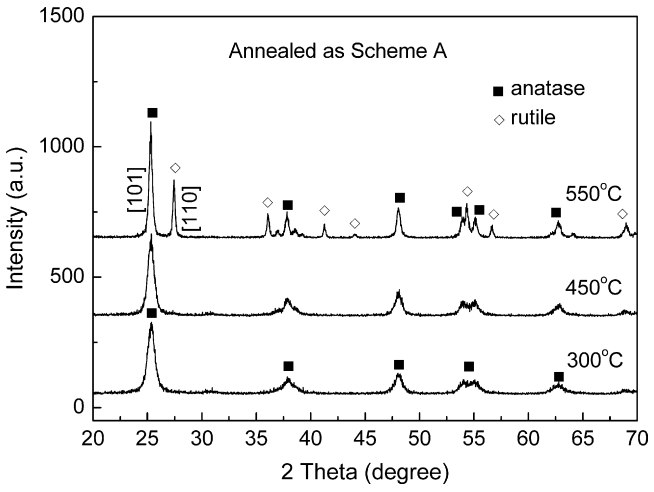

Fig. 3. XRD patterns of the TiO_2 NT-powders annealed by the Scheme A.

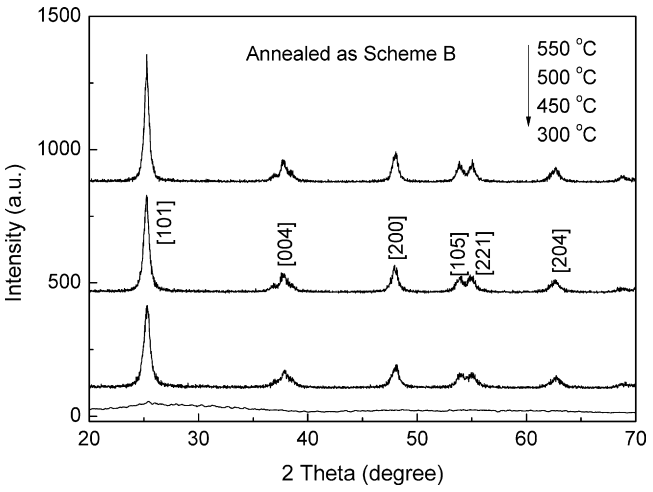

Fig. 5. XRD patterns of the TiO_2 NT-powders annealed by Scheme B.

such as (1 0 1), (0 0 4), (2 0 0) are detected, indicating that the TiO_2 NT-powders are in the pure anatase phase at the heat treatment of 300 °C. For the TiO_2 NT-powders annealed at 450 °C, the TiO_2 NT-powders also only show the anatase characteristic diffraction peaks (JCPDS Patterns No. 21-1272). However, with increase the heat treatment temperature to 550 °C, the characteristic peaks of both the rutile titania and the anatase titania can be observed. These results indicate that the TiO_2 NT-powders are crystallized in anatase phase when they are annealed at 300 °C and 450 °C, while the TiO_2 NT-powders are crystallized into a mixed phase of the anatase and the rutile when annealed at 550 °C. As one knows, the anatase titania and the rutile titania are two polymorphs, and they are typically being used as photocatalysts, but the anatase phase exhibiting higher photocatalytic activity than the rutile phase. One possible explanation is that the anatase phase owns a higher charge-carrier mobility of 80 $cm^2\ V^{-1}\ S^{-1}$, which is 89 times faster than that of the rutile phase [26]. However, the mixture phase of the rutile and the anatase is also expected to be helpful for the photocatalytic performance, because it can facilitate the separation of electron–hole pairs.

The photocatalytic properties of the TiO_2 NT-powders annealed by Scheme A are shown in Fig. 4. It can be seen from the blank test that only 20% of the 20 mg/L MO aqueous solution is photodegraded, indicating that the MO aqueous solution is stable enough as the probe for the investigation of the photocatalytic properties of the TiO_2 NT-powders. With an addition of the TiO_2 NT-powders annealed by Scheme A, the MO aqueous solution is obviously photocatalytic-degraded under UV irradiation within 50 min, and the MO degradation rate is obviously faster than that as observed in the blank test. It is noted that with an increase of the annealing temperature from 300 °C to 550 °C, the photocatalytic activity of the annealed TiO_2 NT-powders also increases. Considering the fact revealed by XRD results that the samples annealed at 300 °C and 450 °C are both in pure anatase phase, but the photocatalytic activity of the TiO_2 NT-powders annealed at 450 °C is better than that of the sample annealed at 300 °C. It is probably attributed to the better crystallization due to a higher heat treatment temperature. It is also noteworthy that the TiO_2 NT-powders annealed at 550 °C show the highest photocatalytic activity, which is probably attributed to the coexistence of the rutile phase and the anatase phase due to a possible effect of the semiconductor–semiconductor junction [24,26]. In addition, the commercial Degussa P-25 powders, which are composed of the anatase–rutile mixed TiO_2 nanocrystallines, are also carried out testing under the same conditions. It is noted that the P-25 powders own a higher photocatalytic activity than the TiO_2 NT-powders obtained under present conditions. One possible explanation is that the P-25 powders can be dispersed in the MO aqueous solution better than the TiO_2 NT-powders do, that is to say, the dispersal ability of the samples will also affect its photocatalytic activity. It can be concluded based on these above results that the TiO_2 NT-powders annealed at 550 °C own the highest photocatalytic activity to the degradation of the MO aqueous solution, namely the optimal temperature for Scheme A is at 550 °C.

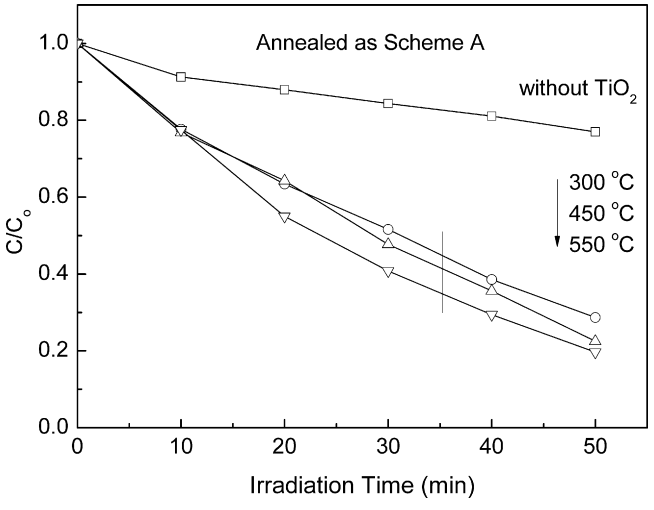

Fig. 4. Photocatalytic degradation kinetics of the MO aqueous solution using the TiO_2 NT-powders annealed by Scheme A and the blank test.

3.3. Crystalline and photocatalytic properties of the TiO_2 NT-powders annealed by Scheme B

Fig. 5 shows the XRD patterns of the TiO_2 NT-powders, which were annealed by Scheme B at 300, 450, 500, and 550 °C. It can be seen that no any diffraction peaks are observed when the sample is annealed at 300 °C, indicating that the TiO_2 NT-powder still stays at amorphous structure. With increase the annealing temperature to 450 °C or above, some diffract peaks located at $2\theta = 25.4°$ (1 0 1), 37.8° (0 0 4), and 48.1° (2 0 0), which can be assigned to the anatase titania (JCPDS Patterns No. 21-1272), can be clearly observed. The (1 0 1) peak of the thermodynamically stable anatase crystal structure in intensity increases as the annealing temperature rises from 450 °C to 550 °C, which indicates an improvement of the crystallization of the anatase phase gradually. It is also interestingly found

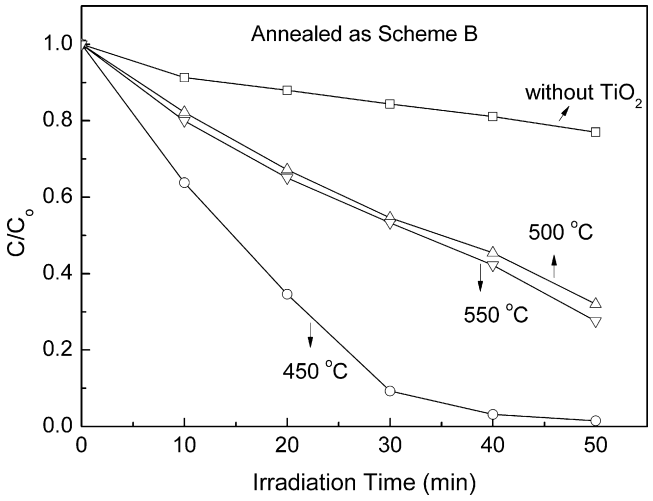

Fig. 6. Photocatalytic degradation kinetics of the MO aqueous solution using the TiO_2 NT-powders annealed by Scheme B.

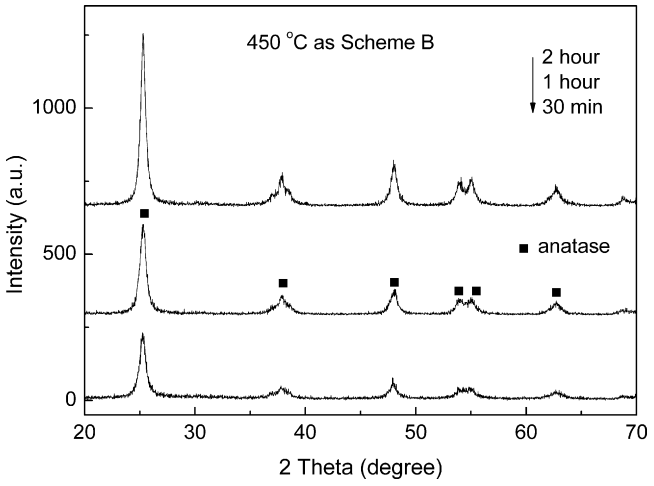

Fig. 7. XRD patterns of the TiO_2 NT-powders annealed at 450 °C by Scheme B under different heat duration.

that the TiO_2 NT-powders annealed at 300 °C by Scheme B is still in amorphous, but they are well crystallized into the anatase phase at 300 °C for the Scheme A as shown in Fig. 3. In addition to, the TiO_2 NT-powders annealed at 550 °C by Scheme A show a mixture phase of the anatase and the rutile, while they are crystallized only still in pure anatase phase at 550 °C for the Scheme B, these results indicate that the phase composition of the annealed TiO_2 NT-powders depend on the scheme of the thermal treatment process. Actually, similar results were also reported by Grimes etc. [27], and they found that the anodized TiO_2 NTs were crystallized into pure anatase after infrared annealing at 600 °C for 15 min and an anatase–rutile mixed phase after thermal annealing at 600 °C for 4 h. Therefore, it can be inferred that different post annealing strategies may greatly affect the crystal structures of the anodized TiO_2 NTs.

The photocatalytic properties of the TiO_2 NT-powders annealed by Scheme B are shown in Fig. 6. It can be seen that the MO aqueous solution can be efficiently photocatalytic-degraded by the TiO_2 NT-powders annealed at 450, 500, and 550 °C. Especially, with the addition of the TiO_2 NT-powders annealed at 450 °C, the MO aqueous solution is completely photocatalytic-degraded until to null within 50 min, while there are still an existence of about 30% residual MO for the TiO_2 NT-powders annealed at 500 °C or 550 °C. These results indicate that the TiO_2 NT-powders annealed at 450 °C have a better photocatalytic activity, and the TiO_2 NT-powders annealed at 500 °C or 550 °C have lower photocatalytic activities as compared with the TiO_2 NT-powders annealed at 450 °C. In order to further explore the photocatalytic activity of the sample annealed at 450 °C by Scheme B, the TiO_2 NT-powders were further studied by changing the heat treatment duration at 450 °C, so as to find out the optimal heat duration. Fig. 7 shows the XRD patterns of the TiO_2 NT-powders annealed at 450 °C with different heat treatment durations. It can be seen that all the samples show similar diffraction peaks, which can be assigned to the anatase phase. As expected, the intensity of the main diffraction peak at $2\theta = 25.4°$ increases with the heat treatment duration rising from 30 min to 2 h. Fig. 8 shows the photocatalytic property of the TiO_2 NT-powders under different heat treatment durations at 450 °C. Results indicate that the photocatalytic activity is obviously improved with increase the heat treatment duration from 30 min to 1 h. However, the photocatalytic activity weakens with further increase the heat treatment duration from 1 h to 2 h. Indicating that the optimal heat treatment duration for achieving the highest photocatalytic activity is 1 h, also the TiO_2 NT-powders annealed at 450 °C for 1 h by the Scheme B own the highest photocatalytic activities for the degradation of the MO aqueous solution. We think that the morphology and nanotubular configuration of the nanotube powders might be also a key factor to affect the photocatalytic activity. The sample annealed at 450 °C for 1 h by Scheme B may be closer to the balance between the crystal phase and the nanotubular configuration. That is to say, an annealing at 450 °C for 1 h not only the TiO_2 NT-powders has a good crystallization but also the nanotubular configuration of the TiO_2 NT-powders can be also maintained well.

Above results indicate that nearly all the samples are well crystallized, but have different photocatalytic degradation activities for the MO aqueous solution. The photocatalytic degradation of the MO aqueous solution can be regarded as a pseudo-first-order reaction [28], and its kinetics can be expressed as follows:

$$C_t = C_o e^{-kt} \quad (2)$$

where k (min^{-1}) is the degradation rate constant and C_t and C_o are the MO concentration at the reaction time t and the initial concentration, respectively. Thus the degradation rate of the annealed samples can be calculated from Eq. (2) and the k values accompanied by crystalline phase are listed in Table 1. It can been seen from Table 1 that for Scheme A, the TiO_2 NT-powders annealed at 550 °C own the highest k value of 0.02970 min^{-1}; for Scheme B,

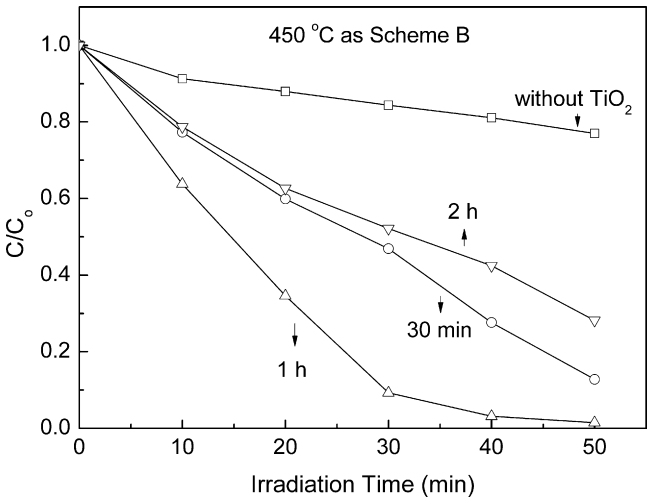

Fig. 8. Photocatalytic degradation kinetics of the MO aqueous solution using the TiO_2 NT-powders annealed at 450 °C by Scheme B under different heat duration.

Table 1
Crystal phases and degradation rate constant k values of the TiO_2 NT-powders after heat treatment.

Heat treatment condition	Crystal phase	k/min^{-1}
300 °C-Scheme A	Anatase	0.02379
450 °C-Scheme A	Anatase	0.02593
550 °C-Scheme A	Anatase + rutile	0.02970
300 °C-Scheme B	Amorphous	–
450 °C-Scheme B	Anatase	0.06973
500 °C-Scheme B	Anatase	0.02045
550 °C-Scheme B	Anatase	0.02233
450 °C-2 h-Scheme B	Anatase	0.02314
450 °C-30 min-Scheme B	Anatase	0.02998

the TiO_2 NT-powders annealed at 450 °C own the highest k value of 0.06973 min^{-1}. The obtained results are consistent with those revealed by Figs. 4, 6 and 8, namely, 550 °C and 450 °C are the optimal annealing temperatures corresponding to Scheme A and Scheme B, respectively.

In order to understand well the two different heat treatment schemes, a comparison between the best photocatalytic activities of the samples annealed by Scheme A (k = 0.02970 min^{-1}) and Scheme B (k = 0.06973 min^{-1}) is carried out as shown in Fig. 9. It is found that the 20 mg/L MO aqueous solution can be completely photocatalytic-degraded under ultraviolet irradiation with the addition of the TiO_2 NT-powders annealed at 550 °C by Scheme A or at 450 °C by Scheme B, but it takes longer time for the best photocatalyst obtained by Scheme A to decompound the MO completely (about 90 min) than the best photocatalyst obtained by Scheme B (about 50 min). Indicating that the TiO_2 NT-powders annealed at 450 °C by Scheme B own much higher photocatalytic activity than the TiO_2 NT-powders annealed at 550 °C by Scheme A. For Scheme A, considering the fact that the TiO_2 NT-powders annealed at 550 °C have higher photocatalytic activity than those samples annealed at 300 °C or 450 °C due to a coexistence of the anatase phase and the rutile phase, but the photocatalytic activity of the TiO_2 NT-powders annealed at 550 °C by Scheme A is not as efficient as that of the TiO_2 NT-powders annealed at 450 °C by Scheme B. We suspect that there should be other factors to affect the photocatalytic activity of the samples except for the crystalline phase. It is widely acknowledged that the morphological and structural factors strongly affect the photocatalytic property of the semiconductor materials since the photoreactivity is directly related to the quantum yield of titania [29]. The higher surface area provides the

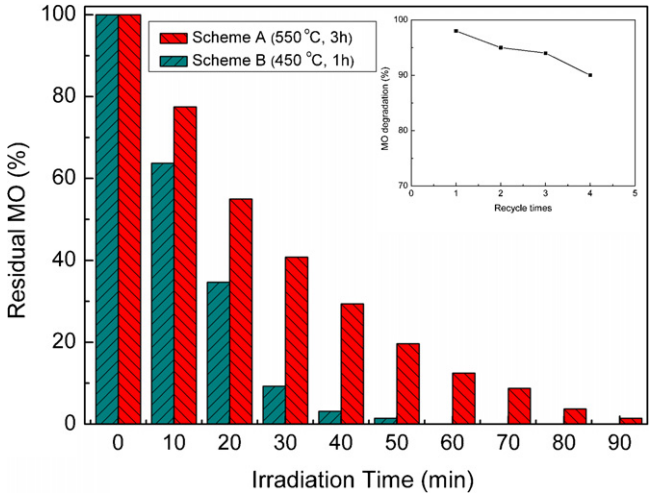

Fig. 9. Photocatalytic activity comparison of the best photocatalyst obtained by Scheme A and Scheme B, respectively and the inset shows a recycling test of the photocatalytic activity of the best sample obtained by Scheme B at 450 °C for 1 h.

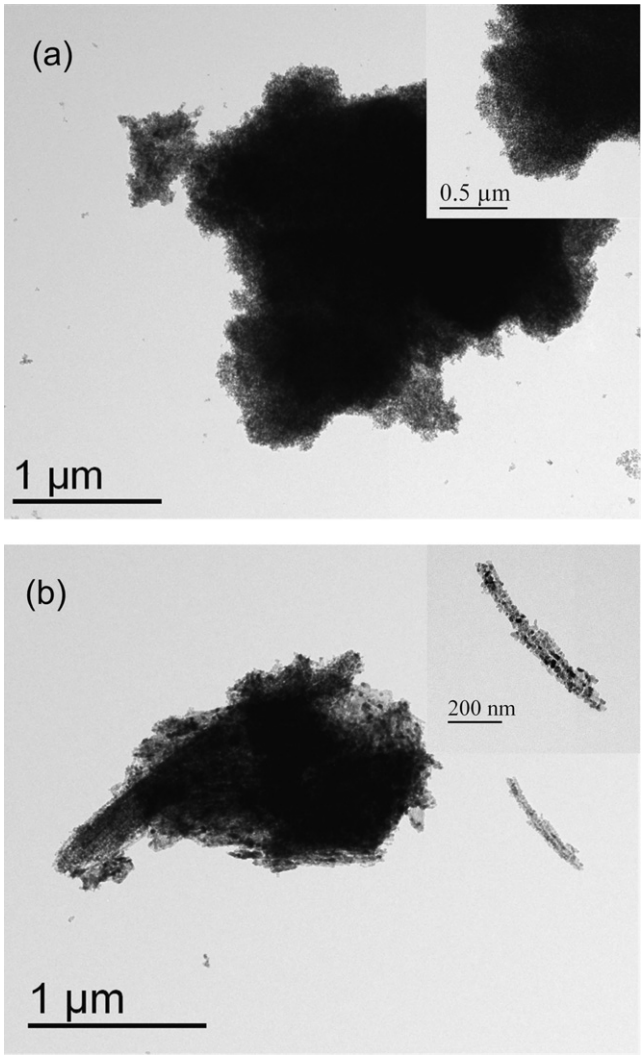

Fig. 10. Typical TEM images of the TiO_2 NT-powders annealed by (a) Scheme A and (b) Scheme B.

catalysts more chances to reach target molecules for degradation and increases catalytic activity. Fig. 10(a) and (b) shows the typical TEM images of the TiO_2 NT-powders annealed by Scheme A and Scheme B, respectively. It can be seen from Fig. 10(a) that the initial nanotubular configuration of the TiO_2 NT-powder has been completely destroyed to become micro particles that consist of the tiny crystal grains. However, the nanotubular structure of the sample annealed by Scheme B is maintained well as shown in Fig. 10(b). As one knows, the nanotubular configuration owns large specific surface area due to both the internal and external areas of the nanotubes, thus it can enhance the adsorption of the MO molecules onto the surface of photocatalyst and subsequently increase the photocatalytic degradation [30]. At the same time, such nanotubular architecture also provides channels for enhanced electron transfer [20]. These two advantages might be the reason why the sample obtained by Scheme B has more efficient photocatalytic activity than the sample obtained by Scheme A. Furthermore, after four times reusing, recycling test of the photocatalytic activity of the best sample obtained by Scheme B at 450 °C for 1 h was also carried out under the same condition and the result is shown as the inset of Fig. 9. It can be seen that its photocatalytic activity decreases a little, namely from 98% to 90% after 50 min UV irradiation, it might be due to the aggregation of the TiO_2 NT-powders with an increase of the recycle times. It can be concluded based on above results and anal-

ysis that the TiO_2 NT-powders with the best photocatalytic activity should have the coexistence of the anatase phase and the rutile phase and remain an ideal nanotubular configuration.

4. Conclusions

The TiO_2 NT-powders have been successfully prepared by the rapid anodization of titanium foil in an aqueous electrolyte containing 0.15 M $HClO_4$ at 25 °C under a constant potential of 20 V. The as-prepared TiO_2 NT-powders show an amorphous phase, and then they are crystallized under two different heat treatment schemes. For Scheme A, the TiO_2 NT-powders are crystallized into an anatase phase from 300 °C to 450 °C and a coexistence of the anatase phase and the rutile phase at 550 °C. The results of the photocatalytic testing indicate that when the annealing temperature is at 550 °C, the TiO_2 NT-powders show the highest photocatalytic activity for degradation of the MO aqueous solution due to the coexistence of the rutile phase and the anatase phase. For Scheme B, the TiO_2 NT-powders are crystallized only in anatase phase from 450 °C to 550 °C, and the optimal annealing temperature for the highest photocatalytic activity is 450 °C, because at this temperature not only the TiO_2 NT-powders has a good crystallization but also the nanotubular configuration of the TiO_2 NT-powders can be maintained well. It is also noted that the TiO_2 NT-powders annealed at 450 °C by Scheme B own much better photocatalytic activity than the TiO_2 NT-powders annealed at 550 °C by Scheme A, indicating that there should be a balance between crystal phase and nanotubular configuration for achieving the best photocatalytic activity of the TiO_2 nanotube powders. These results are expected to be helpful for further understanding of the photocatalytic properties of the TiO_2 NT-powders.

Acknowledgments

This work was supported by the Major Program of the National Natural Science Foundation of China under Grant No. 90923012, the Ministry of Science and Technology of China through 863-project under grant 2009AA03Z218 and the Research Fund for the Doctoral Program of Higher Education of China under grant 200806980023.

References

[1] M.R. Hoffmann, S.T. Martin, W. Choi, D.W. Bahnemann, Chem. Rev. 95 (1995) 69–96.
[2] A. Bravo, J. Garcia, X. Domenech, J. Peral, J. Chem. Res. (1993) 376–377.
[3] J.M. Macak, M. Zlamal, J. Krysa, P. Schmuki, Small 3 (2007) 300–304.
[4] I.P. Parkin, R.G. Palgrave, J. Mater. Chem. 15 (2005) 1689–1695.
[5] R. Hahn, J.M. Macak, P. Schmuki, Electrochem. Commun. 9 (2007) 947–952.
[6] Y.K. Lai, Y.C. Chen, Y.X. Tang, D.G. Gong, Z. Chen, C.J. Lin, Electrochem. Commun. 11 (2009) 2268–2271.
[7] A. Mills, A. Lepre, N. Elliot, S. Bhopal, I.P. Parkin, S.A. O'Neill, J. Photochem. Photobiol. A: Chem. 160 (2003) 213–224.
[8] Y.X. Tang, Y.K. Lai, D.G. Gong, K.H. Goh, T.T. Lim, Z.L. Dong, Z. Chen, Chem. Eur. J. 16 (2010) 7704–7708.
[9] Y.K. Lai, H.F. Zhuang, K.P. Xie, G.G. Gong, Y.X. Tang, L. Sun, C.J. Lin, Z. Chen, New J. Chem. 34 (2010) 1335–1340.
[10] S. Berger, A. Ghicov, Y.C. Nah, P. Schmuki, Langmuir 25 (2009) 4841–4844.
[11] A. Rampaul, I.P. Parkin, S.A. O'Neill, J. DeSouza, A. Mills, N. Elliott, Polyhedron 22 (2003) 35–44.
[12] Z. Ma, Y.H. Yue, X.Y. Deng, Z. Gao, J. Mol. Catal. A: Chem. 78 (2002) 97–104.
[13] M.A. Khan, H.T. Jung, O.B. Yang, J. Phys. Chem. B 110 (2006) 6626–6630.
[14] Y.S. Chen, J.C. Crittenden, S. Hackney, L. Sutter, D.W. Hand, Environ. Sci. Technol. 39 (2005) 1201–1208.
[15] H.C. Liang, X.Z. Li, J. Hazard. Mater. 162 (2009) 1415–1422.
[16] D.A. Wang, Y. Liu, B. Yu, F. Zhou, W.M. Liu, Chem. Mater. 21 (2009) 1198–1206.
[17] D.S. Seoa, J.K. Lee, H. Kimb, J. Cryst. Growth 229 (2001) 428–432.
[18] J.J. Qiu, W.D. Yu, X.D. Gao, X.M. Li, Nanotechnology 17 (2006) 4695–4698.
[19] J.H. Jung, H. Kobayashi, K.J.C. Bommel, S.J. Shinkai, T. Shimizu, Chem. Mater. 14 (2002) 1445–1447.
[20] N.F. Fahim, T. Sekino, Chem. Mater. 21 (2009) 1967–1979.
[21] Y.L. Liao, W.X. Que, J. Alloys Compd. 505 (2010) 243–248.
[22] Y.S. Sohn, Y.R. Smith, M. Misra, V. Subramanian, Appl. Catal. B: Environ. 84 (2008) 372–378.
[23] K. Varghese, D.W. Gong, M. Paulose, C.A. Grimes, E.C. Dickey, J. Mater. Res. 18 (2003) 156–165.
[24] B. Xia, H.Z. Huang, Y.C. Xie, Mater. Sci. Eng. B 57 (1999) 150–154.
[25] J.D.J. Ingle, S.R. Crouch, Spectrochemical Analysis, Prentice Hall, New Jersey, 1988.
[26] S. Bakardjieva, J. Subrt, V. Stengl, M.J. Dianez, M.J. Sayagues, Appl. Catal. B: Environ. 58 (2005) 193–202.
[27] N.K. Allam, C.A. Grimes, J. Phys. Chem. C 113 (2009) 7996–7999.
[28] A.Z. Abdullah, P.Y. Ling, J. Hazard. Mater. 173 (2010) 159–167.
[29] Y. Zheng, E. Shi, Z. Chen, W. Li, X. Hu, J. Mater. Chem. 11 (2001) 1547–1551.
[30] S. Malato, J. Blanco, A. Vidal, C. Richter, Appl. Catal. B: Environ. 37 (2002) 1–15.